NANO LETTERS

2003
Vol. 3, No. 9
1203−1207

Nanostructured Electrochemical Sensor Based on Dense Gold Nanoparticle Films

Aimin Yu,[†] Zhijian Liang,[†] Jinhan Cho,[‡] and Frank Caruso*[,‡]

Max Planck Institute of Colloids and Interfaces, Potsdam 14464, Germany, and Department of Chemical and Biomolecular Engineering, The University of Melbourne, Victoria 3010, Australia

Received June 1, 2003; Revised Manuscript Received June 23, 2003

ABSTRACT

Polyelectrolyte (PE)/gold nanoparticle hybrid films that can be utilized as efficient electrochemical sensors were prepared by infiltrating 4-(dimethylamino)pyridine-stabilized gold nanoparticles (DMAP−Au_{NP}) into PE multilayers preassembled on indium tin oxide (ITO) electrodes. Quartz crystal microgravimetry (QCM) and UV−vis spectroscopy showed that via this infiltration method, composite films with densely packed DMAP−Au_{NP} were obtained. Electrochemical experiments revealed that the presence of gold nanoparticles in the PE multilayers could significantly improve the electron-transfer characteristics of the films, which showed high electrocatalytic activity to the oxidation of nitric oxide (NO). The sensitivity of the composite films for measuring NO could be further tailored by controlling the gold nanoparticle loading in the film.

Metal nanoparticles have attracted extensive interest because of their unique electronic, optical, and catalytic properties. The integration of metal nanoparticles into thin films is particularly important for various applications, for example, in biological sensing and in the preparation of optoelectronic nanodevices.[1−5] The use of gold nanoparticle building blocks for the creation of electrochemical sensing devices is also promising.[3,6−10] Although gold is a poor catalyst in bulk form, nanometer-sized gold nanoparticles can exhibit excellent catalytic activity due to their relative high surface area-to-volume ratio, and their interface-dominated properties, which significantly differ from their bulk counterparts.[11−13] Haruta and co-workers have demonstrated that gold nanoparticles (<10 nm) supported on oxides display high catalytic activity for the chemical and electrochemical oxidation of carbon monoxide (CO) and methanol.[14] Goodman and co-workers reported that the high catalytic activity of gold nanoparticles in catalyzing CO oxidation is related to the band gap of a metallic-insulator transition for particles in the range of a few nanometers.[15]

The preparation of thin films with a high density of metal nanoparticles is often desired for catalysis and electronics.[2] Films of close-packed metal nanoparticles can be achieved via self-assembly of metal nanoparticles from organic media onto solid supports.[16−18] However, the formation of dense films of metal nanoparticles from aqueous nanoparticle dispersions is often difficult to obtain.[19−21] Previous reports showed that the surface coverage of gold nanoparticles adsorbed from aqueous solution onto substrates is less than about 30%.[20,22,23] A common approach to increase the nanoparticle loading on surfaces includes using additional linker molecules to bind extra nanoparticles to the surface.[19,22,24] However, from a catalysis viewpoint, the disadvantage of this method is that the typically covalently bound molecules will adversely affect the catalytic reactivity of the nanoparticles.[25] Recently, we demonstrated that metallic-composite films comprising a dense packing of gold nanoparticles can be achieved by infiltrating gold nanoparticles stabilized by the ligand 4-(dimethylamino)pyridine (DMAP−Au_{NP}) into preformed poly(sodium 4-styrenesulfonate) (PSS) and poly(allylamine hydrochloride) (PAH) multilayer films.[26] The nature of the adsorbed ligand as well as the polyelectrolyte (PE) adsorption matrix resulted in the formation of dense nanoparticulate films.[26] Unlike many other ligand-capped metal nanoparticle systems where the ligand is covalently attached (e.g., thiol-stabilized nanoparticles), DMAP can be readily removed from the gold nanoparticle surface through water rinsing.[27] This is an important feature of the DMAP−Au_{NP} system with regard to catalysis applications. In this paper, we investigate the utility of these PE/Au_{NP} composite films in electrocatalysis. The focus of this work is to study the electron-transfer characteristics of Au nanoparticles in PE multilayers, and the capacity of such films (with varying gold nanoparticle loadings) to act as electrochemical sensors.

* Corresponding author. Fax: +61 3 8344 4153. E-mail: fcaruso@unimelb.edu.au.
[†] Max Planck Institute.
[‡] The University of Melbourne.

10.1021/nl034363j CCC: $25.00
Published on Web 08/12/2003

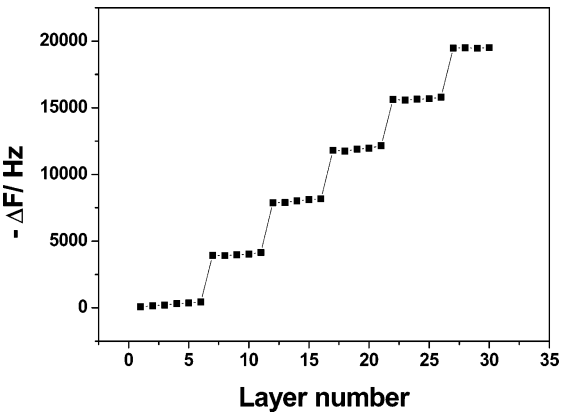

Figure 1. Frequency change as a function of the number of layers for the assembly of a PE/DMAP−Au_{NP} film on a QCM electrode. The large frequency changes (layers 7, 12, 17, 22, and 27) correspond to DMAP−Au_{NP} deposition. The first layer deposited was PEI. One cycle of six layers corresponds to $(PSS/PAH)_2/PSS/Au_{NP}$.

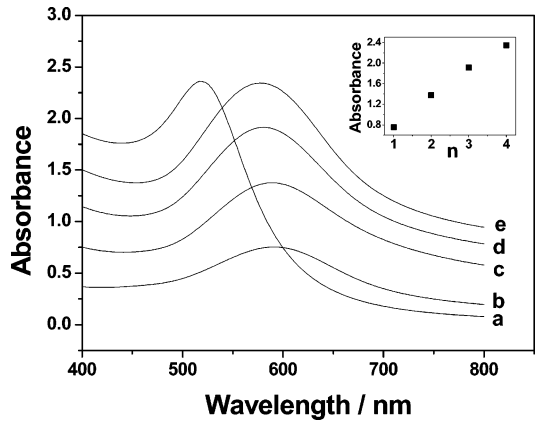

Figure 2. UV−vis absorption spectra of a DMAP−Au_{NP} dispersion (a) and films of $PEI/(PSS/PAH)_2/PSS/Au_{NP}$ (b), $PEI/[(PSS/PAH)_2/PSS/Au_{NP}]_2$ (c), $PEI/[(PSS/PAH)_2/PSS/Au_{NP}]_3$ (d), and $PEI/[(PSS/PAH)_2/PSS/Au_{NP}]_4$ (e) on ITO substrates. The inset shows that the absorbance maximum increases with the number of DMAP−Au_{NP} deposition cycles (n).

The PE multilayer films used as matrices for DMAP−Au_{NP} infiltration were prepared by first adsorbing poly(ethylenimine) (PEI) onto a solid support (gold, silicon or ITO), followed by five alternating layers of PSS and PAH through the layer-by-layer (LbL) technique.[28] The first layer of PEI was used as a primer layer. The negatively charged, outermost layer (PSS) was exploited for adsorbing the positively charged DMAP−Au_{NP}. The PE-modified substrates were immersed into the gold nanoparticle dispersion for 60 min and washed with pure water. Thicker composite films were obtained by repeatedly depositing five layers of PE and gold nanoparticles [i.e., $(PSS/PAH)_2/PSS/Au_{NP}$].

We first used QCM to quantitatively characterize the formation of PE/gold nanoparticle composite films. Figure 1 shows the frequency changes associated with the formation of the films on QCM electrodes. Infiltration of DMAP−Au_{NP} into the PE films resulted in a significant decrease in the QCM frequency: the average frequency change for a single deposition of DMAP−Au_{NP} is ca. 3600 (± 580) Hz, which corresponds to ∼3150 ng[29] or $\sim 4.5 \times 10^{12}$ particles cm^{-2}. A surface coverage of $\sim 2.8 \times 10^{12}$ particles cm^{-2} is expected, assuming the gold nanoparticles (6 nm diameter) form a nanoparticle layer in a 2D hexagonal close packing structure (surface coverage ratio of 74%). The similar frequency changes for the DMAP−Au_{NP} adsorption steps indicate that similar amounts of nanoparticles were deposited with each adsorption step (within ∼15%). The QCM results indicate that the DMAP−Au_{NP} surface coverage (per deposition) is approximately 1.6 times that expected for a close-packed, monolayer nanoparticle coverage. As we reported earlier,[26] the dense packing of nanoparticles in the film is attributable to the reversible binding nature of the DMAP ligand stabilizing the gold nanoparticles and the PE matrix used to immobilize the gold nanoparticles. After infiltrating DMAP−Au_{NP} into the PE films and washing with water, it is postulated that DMAP is removed from the gold nanoparticle surface[26] (hence, in the films the nanoparticles are denoted Au_{NP}) and that the nanoparticles are stabilized by the PE chains; for example, via weak covalent bonding with the uncharged amine groups of PAH.[30] It is possible that some residual DMAP may be present in the films.

The deposition of successive PE/gold nanoparticle layers was further characterized by UV−vis spectroscopy. Figure 2, curve a, shows the UV−vis spectrum of the DMAP−Au_{NP} dispersion. The surface plasmon absorption peak is located at 517 nm. Following the sequential deposition of multilayer films on ITO using the same procedure used to prepare the films on QCM electrodes, the surface plasmon resonance peak position shifted to about 590 nm (Figure 2, curve b). The red-shift of the surface plasmon is due to a reduced nanoparticle−nanoparticle distance (i.e., more dense packing) in the film as compared with DMAP−Au_{NP} dispersed in water,[31,32] and also due to the change of the refractive index as a result of the surrounding PE matrix.[33] It is also noted that with increasing the film thickness, no further broadening of the surface plasmon absorption band occurs, but a systematic blue shift in the peak maximum occurs. Compared with the maximum absorption wavelength of 590 nm (curve b) for the first "gold nanoparticle layer", the maximum absorption wavelength of the "fourth nanoparticle layer" shifted to 577 nm (curve e), i.e., ∼13 nm blue shift. This indicates that the average nanoparticle−nanoparticle distance increases with increasing film thickness, which may be explained by variations in the layer structure and/or nanoparticle loading. Despite such a blue shift the maximum absorbance increases regularly with the number of deposited DMAP−Au_{NP} layers (Figure 2, inset).

The surface morphology of a PE/Au nanoparticle hybrid film was investigated by atomic force microscopy (AFM). Figure 3 shows AFM images of a $PEI/(PSS/PAH)_2/PSS$ multilayer film assembled on a silica substrate before (a) and after (b) exposure to a DMAP−Au_{NP} dispersion. The PE film on the silica surface is rather smooth, with a root-mean-squared (RMS) roughness of ∼1 nm. After infiltration of the gold nanoparticles, the film becomes considerably rougher (RMS ∼6 nm). AFM tip convolution effects magnify the observed diameters of the nanoparticles (∼20−70 nm).

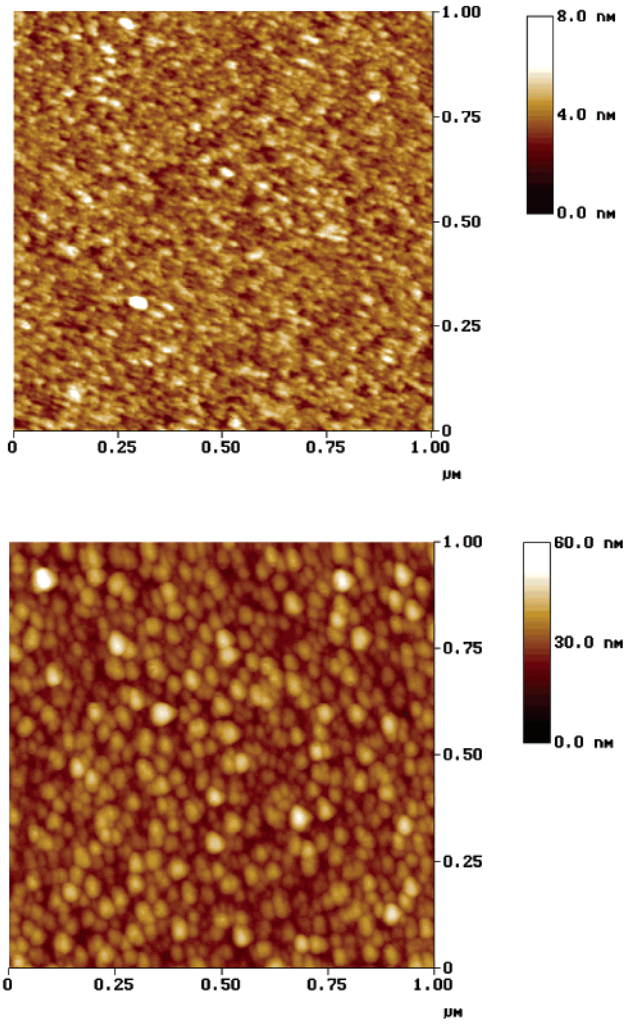

Figure 3. AFM images of a PEI/$(PSS/PAH)_2$/PSS film before (a) and after (b) infiltration of DMAP−Au_{NP}.

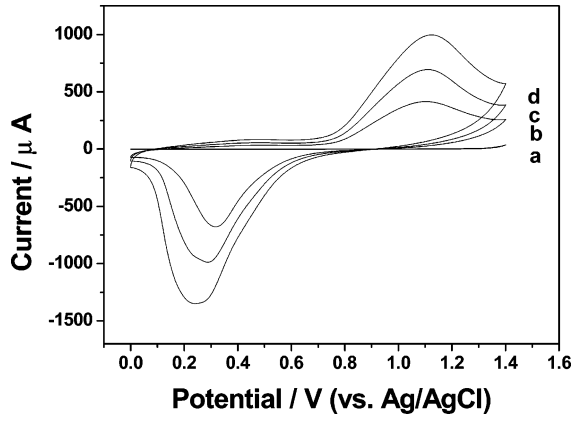

Figure 4. Cyclic voltammograms of a bare ITO electrode (a), and ITO electrodes modified with PEI/$(PSS/PAH)_2$/PSS/Au_{NP} (b), PEI/$[(PSS/PAH)_2/PSS/Au_{NP}]_2$ (c), and PEI/$[(PSS/PAH)_2/PSS/Au_{NP}]_3$ (d) in pH 7.0 PBS. Scan rate = 50 mV/s.

The films prepared were examined for electrochemical activity. Figure 4, curves b−d, show the cyclic voltammograms (CVs) of the composite films with various layers of gold nanoparticles in pH 7.0 phosphate buffer solution (PBS). It can be seen that in the potential region from 0 to 1.3 V there is an oxidation peak at ~1.1 V and a reduction peak at ~0.3 V. As bare ITO electrodes (Figure 4, curve a) and PE multilayer-modified electrodes (data not shown) have no current response in this potential region, the redox peaks are attributed to the oxidation and subsequent reduction of surface gold oxide (AuO_x) formation on the gold nanoparticles as a result of the positive potential polarization.[34,35] These data are indicative of the presence of gold nanoparticles and the chemical reversibility of the surface reaction. With thicker films (i.e., a higher gold nanoparticle content), the redox peaks of Au increase (Figure 4, curves c,d). It can also be noted that the reduction potential of gold becomes slightly negatively shifted with increasing gold nanoparticle content because of the increasing difficulty for the electron-transfer reaction between the gold nanoparticles and the electrode with increasing film thickness.

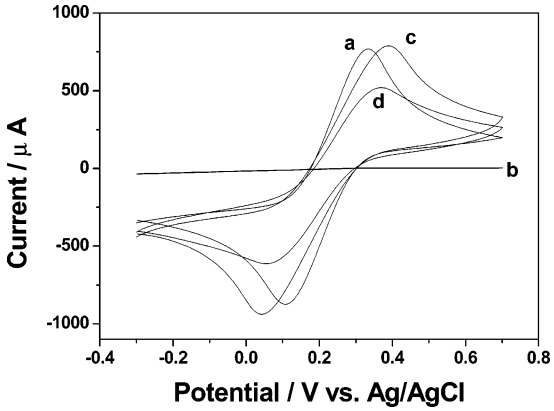

Figure 5. Cyclic voltammograms of 10 mM $K_3Fe[CN]_6$ in pH 7.0 PBS at a bare ITO electrode (a), and ITO electrodes modified with PEI/$(PSS/PAH)_2$/PSS (b), PEI/$(PSS/PAH)_2$/PSS/Au_{NP} (c), and PEI/$[(PSS/PAH)_2/PSS/Au_{NP}]_3$ (d). Scan rate = 50 mV/s.

To examine the electronic communication behavior between the immobilized gold nanoparticles and the electrode, we investigated the electrochemical behavior of $K_3Fe[CN]_6$ at the PE/gold nanoparticle film-coated ITO surface. $K_3Fe[CN]_6$ is a substance that undergoes reversible electrochemical reaction on various electrodes and is widely used as an electrochemical probe to investigate the characteristics of films on electrode surfaces.[36,37] Figure 5a shows the CV of $K_3Fe[CN]_6$ at bare ITO electrodes in pH 7.0 PBS. The data show an almost reversible electrochemical response for $K_3Fe[CN]_6$. The peak separation (ΔE_p, the potential difference between the oxidation peak potential and the reduction peak potential, which is inversely proportional to the electron-transfer rate[38]) is 232 mV at 50 mV s^{-1} on bare ITO. After coating the ITO electrode with six layers of PEs (PEI(PSS/$PAH)_2$PSS), there is no visible current response for $K_3Fe[CN]_6$ (curve b) due to the sluggish electron-transfer kinetics through the PE film.[36,37] However, after infiltration of gold nanoparticles into the PE multilayer film, almost reversible CVs of $K_3Fe[CN]_6$ are seen (Figure 5, curve c), with nearly the same current response and a slightly larger ΔE_p (350 mV) compared with that obtained for the bare electrode. Nearly reversible CVs were obtained for the electrode prepared via three infiltration cycles of DMAP−Au_{NP} (Figure 5, curve d). It is noted that this electrode has 16 layers of

PE on the surface. This is in stark contrast to six-layer PE-coated electrode (Figure 5, curve b), which shows no electrochemical response. This reveals that the gold nanoparticles in the PE layers improve the electron transfer between $K_3Fe[CN]_6$ and the electrode. The results also provide evidence for infiltration of DMAP−Au_{NP} into the entire film. Although the nanoparticles are likely stabilized by the PE chains, they act as "electron antennae", effectively facilitating electron transfer throughout the film.

Nitric oxide (NO) is a neuronal signal in the central nervous system. The discoveries made in the 1980s that NO could be synthesized by mammalian cells and could act as a physiological messenger and cytotoxic agent elevated the importance of its detection.[39,40] Among the various methods for measuring NO, electrochemical techniques are of great significance not only in that they are direct, simple and rapid, but also in that they are applicable in vivo.[41,42] Here, we use sodium nitrite ($NaNO_2$) as a precursor of NO to investigate the electrocatalytic activity of gold nanoparticles in the PE multilayers.

In acid solution (pH < 4), $NaNO_2$ can generate free NO by the following disproportionation reaction:[43,44]

$$3HONO \rightarrow H^+ + NO_3^- + 2NO + H_2O$$

Successive addition of a stock nitrite solution into the bulk solution was made to generate a series of concentrations of NO. At a bare ITO electrode, there is nearly no response for NO (Figure 6A, curve a). In contrast, at a DMAP−Au_{NP} infiltrated PE-precoated electrode, a new oxidation peak appears at ~0.82 V and the peak current increases with increasing concentration of $NaNO_2$ (Figure 6A, curves b−h), which suggests that the nanoparticles are catalytic to the oxidation of NO. Similar electrocatalytic behavior of NO at a platinum electrode modified by a monolayer of gold nanoparticles and Nafion was recently reported by Jin and co-workers.[45] The suggested electrocatalytic oxidation mechanism is that NO in solution first loses an electron to form NO^+ with the help of Au nanoparticles at the electrode surface. The formed NO^+ can then be further oxidized to form other more stable nitrogen products.[46]

Figure 6B compares two calibration curves corresponding to the amperometric responses of two films, PEI/$(PSS/PAH)_2$/PSS/Au_{NP} and PEI/$[(PSS/PAH)_2$/PSS/$Au_{NP}]_3$, assembled on ITO electrodes. The film prepared with three cycles of DMAP−Au_{NP} deposition has a higher response than that prepared from a single DMAP−Au_{NP} deposition for the same concentration of $NaNO_2$, which suggests that the sensitivity of the sensor can be controlled through the film thickness, or more specifically the gold nanoparticle content in the film. For the electrode coated with PEI/$[(PSS/PAH)_2$/PSS/$Au_{NP}]_3$, a linear dependence of the peak current on the nitrite concentration in the range from 0.05 to 0.5 mM is obtained and the detection limit is about 0.010 mM $NaNO_2$ when using cyclic voltammetry. This value is lower than that previously reported for hemoglobin-based NO sensors (0.10 mM[47], 0.018 mM[48]), which also employ acidic nitrite as a source of NO.

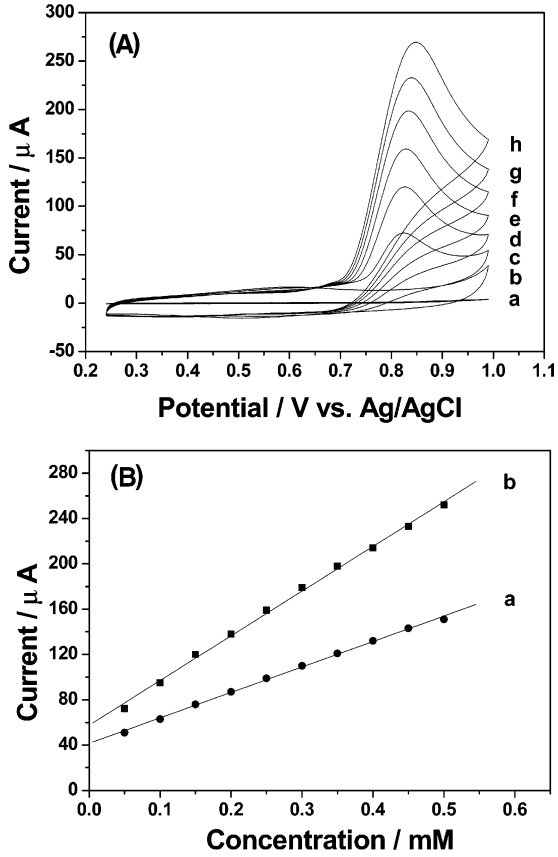

Figure 6. (A) Cyclic voltammograms of a bare ITO electrode in (a) pH 2.0 PBS containing 0.5 mM $NaNO_2$, and a PEI/$[(PSS/PAH)_2$/PSS/$Au_{NP}]_3$-modified electrode in pH 2.0 PBS containing (b) 0, (c) 0.05, (d) 0.15, (e) 0.25, (f) 0.35, (g) 0.45, and (h) 0.55 mM $NaNO_2$. Scan rate = 50 mV/s. (B) Calibration curves of the amperometric responses of ITO electrodes modified with PEI/$(PSS/PAH)_2$/PSS/Au_{NP} (a) and PEI/$[(PSS/PAH)_2$/PSS/$Au_{NP}]_3$ (b) to different concentrations of $NaNO_2$.

In summary, we have demonstrated the preparation of films comprising a dense packing of gold nanoparticles by infiltrating DMAP−Au_{NP} into PE multilayer precursor films. The nanoparticle amount on the modified substrates increases regularly with the number of deposited DMAP−Au_{NP} layers. The presence of gold nanoparticles greatly improves the conductivity and the electron transfer ability of the film. Additionally, the electronic and catalytic properties of the gold nanoparticles can be exploited to utilize the films for the electrochemical detection of NO. The sensitivity of the films is dependent on the gold nanoparticle content, thus providing an alternative means for tuning their electrocatalytic activity, which can be easily controlled through variation of the Au_{NP} loading. With the rapid developments in nanoparticle preparation, surface modification, and assembly, the emergence of novel applications of these and other nanoparticle-related films are likely to impact the areas of sensing, catalysis, and optoelectronics.

Acknowledgment. This work was funded by the German Federal Ministry of Education, Science, Research and Technology (BMBF) Biofuture initiative, the Australian Research Council within the Federation Fellowship and

Discovery Project schemes, and the Victorian State Government, Department of Innovation, Industry and Regional Development, Science, Technology and Innovation initiative. H. Möhwald is acknowledged for support of the work within the MPI Interface Department, and the Particulate Fluids Processing Centre (The University of Melbourne) for infrastructure support. A. Heilig (MPI) is thanked for assistance with the AFM measurements.

References

(1) Cao, Y. W. C.; Jin, R. C.; Mirkin, C. A. *Science* **2002**, *297*, 1536.
(2) Niemeyer, C. M. *Angew. Chem., Int. Ed.* **2001**, *40*, 4128.
(3) Shipway, A. N.; Katz, E.; Willner, I. *Chem. Phys. Chem.* **2000**, *1*, 18.
(4) Kamat, P. V. *J. Phys. Chem. B* **2002**, *106*, 7729.
(5) Shenton, W.; Davis, S. A.; Mann, S. *Adv. Mater.* **1999**, *11*, 449.
(6) Xiao, Y.; Patolsky, F.; Katz, E.; Hainfeld, J. F.; Willner, I. *Science* **2003**, *299*, 1877.
(7) Willner, I.; Willner, B. *Pure. Appl. Chem.* **2001**, *73*, 535.
(8) Wang, J.; Xu, D. K.; Kawde, A. N.; Polsky, R. *Anal. Chem.* **2001**, *73*, 5576.
(9) Gu, H. Y.; Yu, A. M.; Chen, H. Y. *J. Electroanal. Chem.* **2001**, *516*, 119.
(10) Zhang, Y. R.; Asahina, S.; Yoshihara, S.; Shirakashi, T. *Electrochim. Acta* **2003**, *48*, 741.
(11) Henglein, A. *Chem. Rev.* **1989**, *89*, 1861.
(12) Brus, L. *Appl. Phys. A* **1991**, *53*, 465.
(13) Shipway, A. N.; Lahav, M.; Willner, I. *Adv. Mater.* **2000**, *12*, 993.
(14) Biswas, P. C.; Nodasaka, Y.; Haruta, M. *J. Electroanal. Chem.* **1995**, *381*, 167.
(15) Valden, M.; Lai, X.; Goodman, D. W. *Science* **1998**, *281*, 1647.
(16) Whetten, R. L.; Khoury, J. T.; Alvarez, M. M.; Murthy, S.; Vezmar, I.; Wang, Z. L.; Stephens, P. W.; Cleveland, C. L.; Luedtke, W. D.; Landman U. *Adv. Mater.* **1996**, *8*, 428.
(17) Murry, C. B.; Kagan, C. R. *Annu. Rev. Mater. Sci.* **2000**, *30*, 545.
(18) Brust, M.; Kiely, C. J. *Colloids Surf. A* **2002**, *202*, 175.
(19) Musick, M. D.; Keating, C. D.; Keefe, M.; Natan, M. J. *Chem. Mater.* **1997**, *9*, 1499.
(20) Schmitt, J.; Decher, G.; Dressick, W. J.; Brandow, S. L.; Geer, R. E.; Shashidhar, R.; Calvert, J. M. *Adv. Mater.* **1997**, *9*, 61.
(21) Ji, T.; Lirtsman, V. G.; Avny, Y.; Davidov, D. *Adv. Mater.* **2001**, *13*, 1253.
(22) Musick, M. D.; Keating, C. D.; Lyon, L. A.; Botsko, S. L.; Pena, D. J.; Holliway, W. D.; McEvoy, T. M.; Natan, M. J. *Chem. Mater.* **2000**, *12*, 2869.
(23) Ung, T.; Liz-Marzan, L. M.; Mulvaney, P. *J. Phys. Chem. B* **2001**, *105*, 3441.
(24) Wuelfing, W. P.; Zamborini, F. P.; Templeton, A. C.; Wen, X.; Yoon, H.; Murray, R. W. *Chem. Mater.* **2001**, *139*, 87.
(25) Boennemann, H.; Brinkmann, R.; Neiteler, P. *Appl. Organomet. Chem.* **1994**, *8*, 361.
(26) Gittins, D. I.; Susha, A. S.; Schoeler, B.; Caruso, F. *Adv. Mater.* **2002**, *14*, 508.
(27) Gittins, D. I.; Caruso, F. *Angew. Chem., Int. Ed. Engl.* **2001**, *40*, 3001.
(28) Poly(allylamine hydrochloride) (PAH), M_w 70 000; poly (sodium 4-styrene-sulfonate (PSS), M_w 70 000; and poly(ethylenimine) (PEI), M_w 25 000 were obtained from Sigma-Aldrich and PAH and PEI were used as received. PSS was dialyzed against Milli-Q water (M_w cutoff 14 kDa) and lyophilized before use. 9-MHz QCM electrodes (Kyushu Dentsu, Japan) were cleaned by dropping Piranha solution (one part 30% H_2O_2 to three parts 98% H_2SO_4, note the mixture is dangerous as it violently reacts with organics) on both sides of the electrodes (three times for 1 min), followed by extensive rinsing with Mill-Q water. ITO ($R_{est} = 10 \pm 2\ \Omega$, Delta Technologies, USA) and silicon wafers (Silchem Handelsgesellschaft mbH, Germany) were cleaned by using the RCA protocol (i.e., by immersing them in a 5:1:1 (vol %) $H_2O/H_2O_2/NH_3$ mixture at 70 °C for ca. 10 min), followed by extensive rinsing with Milli-Q water. All PE solutions used contained 1 mg mL^{-1} of PE and 0.5 M NaCl. Each layer was prepared by dipping the substrates in PE solution for 15 min, followed by dipping in water (three times for 1 min), and drying with a gentle stream of N_2.
(29) Sauerbrey, G. Z. *Phys.* **1959**, *155*, 206.
(30) Leff, D. V.; Brandt, L.; Heath, J. R. *Langmuir* **1996**, *12*, 4723.
(31) Mirkin, C. A.; Letsinger, R. L.; Mucic, R. C.; Storhoff, J. J. *Nature* **1996**, *382*, 607.
(32) Brust, M.; Bethell, D.; Kiely, C. J.; Schiffrin, D. J. *Langmuir* **1998**, *14*, 5425.
(33) Schmitt, J.; Mächtle, P.; Eck, D.; Möhwald, H.; Helm, C. A. *Langmuir* **1999**, *15*, 3256.
(34) Burke, L. D.; Cunnane, V. J. *J. Electroanal. Chem.* **1986**, *210*, 69.
(35) Burke, L. D.; Nugent, P. F. *Gold Bull.* **1998**, *31*, 39.
(36) Harris, J. J.; Bruening, M. L. *Langmuir* **2000**, *16*, 2006.
(37) Pardo-Yissar, V.; Katz, E.; Lioubashevski, O.; Willner, I. *Langmuir* **2001**, *17*, 1110.
(38) Bard, A. J.; Faulkner, C. R. *Electrochemical Methods: Fundamentals and Applications*, 2nd ed.; John Wiley & Sons Inc.: New York, 2000.
(39) Ignarro, L. J.; Bugga, G. M.; Wood, K. S.; Byrns, R. E.; Chaudhuri, G. *Proc. Natl. Acad. Sci. U.S.A.* **1987**, *84*, 9265.
(40) Koshland, D. E. *Science* **1992**, *258*, 1861.
(41) Shibuki, K. *Neurosci. Res.* **1990**, *9*, 69.
(42) Malinski, T.; Taha, Z. *Nature* **1992**, *358*, 676.
(43) Stedman, G. *Adv. Inorg. Chem. Radiochem.* **1979**, *22*, 113.
(44) Cotton, F. A.; Wilkinson, G. *Advanced Inorganic Chemistry*, 5th ed.; Wiley: New York, 1988; p 327.
(45) Zhu, M.; Liu, M.; Shi, G.; Xu, F.; Ye, X.; Chen, J.; Jin, L.; Jin, J. *Anal. Chim. Acta* **2002**, *455*, 199.
(46) Ciszewski, A.; Milczarek, G.; Kubaszewski, E.; Łożyński, M. *Electroanal.* **1998** *10*, 628.
(47) Yu, A. M.; Zhang, H. L.; Chen, H. Y. *Anal. Lett.* **1997**, *30*, 1013.
(48) Fan, C.; Li, G.; Zhu J.; Zhu, D. *Anal. Chim. Acta* **2000**, *423*, 95.

NL034363J